Modeling and analysis of delaminated beams with integrated piezoelectric actuators

Ali Mahieddine [a,*], Joël Pouget [b], Mohammed Ouali [c]

[a] *Centre universitaire de khemis miliana, route de Théniet El Had, 44225 Khemis Miliana, Ain Defla, Algeria*
[b] *Université Paris 6, 4, place Jussieu, 75005 Paris, France*
[c] *Université Saad Dahleb – Blida, route de Soumaa, Blida, Algeria*

ARTICLE INFO

ABSTRACT

In this article, a mathematical model for beams with partially delaminated layers is presented to investigate their behavior by using Euler–Bernoulli beam theory. The principal advantage of the element is that it allows the modeling of delamination anywhere in the structure. The region without delamination is modeled to carry constant peel and shear stresses; while the region with delamination is modeled by assuming that there is no peel and shear stress transfer between the top and bottom layers. Moreover, in the interfaces between the regions with and without delamination, both displacements and forces continuity conditions are imposed. The accuracy of the models is verified by comparing results with previously published data.

© 2010 Académie des sciences. Published by Elsevier Masson SAS. All rights reserved.

1. Introduction

Vibration and shape control using piezoelectric sensors and actuators have attracted significant attention in recent years. The aspect of vibration control of plates by piezoelectric materials was studied by Yang and Huang [1] and Piéfort et al. [2]. These models are based on the classic theory of laminated plates which neglects the effects of the transverse shear. Finite element model to predict the vibrations of the piezoelectric actuators is presented by Taleghani and Campbell [3]. Basic actuator and sensor equations of composite shell structures with piezoelectric layers are presented by Tzou and Gadre [4] and Tzou [5]. In previous studies, the adhesive layers are not modeled and the fundamental assumption is that the piezoelectric layers are perfectly bonded onto the host structures. Lee et al. [6] studied a composite beam with arbitrary lateral and longitudinal multiple delamination. Finite element methods have been developed using the layerwise theory by Kim et al. [7]. An improved analytical model for delamination in composite beams, using a second-order shear-thickness deformation displacement field, was introduced by Hamed et al. [8]. Tan and Tong [9] developed dynamic analytical model for identification of a delamination embedded in a laminated composite beam. It was noted that the piezoelectric sensor can only effectively identify the size and location of a delamination which is beneath the sensor. Mahieddine and Ouali [10] present a finite element formulation based on the first-order theory of Kirchoff to analyze beams with integrated piezoelectric actuators and sensors.

To investigate the effects of delamination of piezoelectric layers on vibration control of beam, a mathematical model based on Euler–Bernoulli beam theory is developed. The delaminated region of the beam is modeled by assuming that there is no stress between the top and bottom layers. Both displacement continuity and force equilibrium conditions are imposed

---

* Corresponding author.
E-mail addresses: mahieddine.ali@gmail.com (A. Mahieddine), joel.pouget@meca.uvsq.fr (J. Pouget), mo-uali@yahoo.fr (M. Ouali).

Nomenclature

A_B, A_T	Cross-section area of bottom and top layers respectively	u_B', u_T'	First spatial derivatives of u_B and u_T respectively
b	Width of the beam	u_B'', u_T''	Second spatial derivatives of u_B and u_T respectively
$\mathbf{D}$	Electric displacement matrix		
$\mathbf{E}$	Electric field matrix	u_B''', u_T'''	Third spatial derivatives of u_B and u_T respectively
E_z	Electric field relative to z		
$\bar{\mathbf{e}}$	Piezoelectric stress coefficient matrix	$\ddot{u}_B, \ddot{u}_T$	Second time derivatives of u_B and u_T respectively
$\bar{\mathbf{g}}$	Permittivity constant matrix		
h_B, h_T	Thickness of bottom and top layers respectively	w_B, w_T	Displacements, of bottom and top layers respectively, relative to z
k	Parameter characterizing the bonding conditions	w_B', w_T'	First spatial derivatives of w_B and w_T respectively
L	Beam's length	w_B'', w_T''	Second spatial derivatives of w_B and w_T respectively
M_B, M_T	Bending moments of bottom and top layers respectively		
M_B', M_T'	First spatial derivatives of M_B and M_T respectively	w_B''', w_T'''	Third spatial derivatives of w_B and w_T respectively
P	Load per unit length	w_B'''', w_T''''	Fourth spatial derivatives of w_B and w_T respectively
Q_B, Q_T	Transverse shear forces of bottom and top layers respectively		
Q_B', Q_T'	First spatial derivatives of Q_B and Q_T respectively	$\ddot{w}_B, \ddot{w}_T$	Second time derivatives of w_B and w_T respectively
$\bar{O}$	Elastic stiffness	z	Spatial coordinate
T_B, T_T	Axial stress resultants of bottom and top layers respectively	$\varepsilon_B, \varepsilon_T$	Strains for bottom and top layers respectively
		ν	Natural frequency
T_B', T_T'	First spatial derivatives of T_B and T_T respectively	σ	Peel stress
		ρ_B, ρ_T	Mass densities of bottom and top layers respectively
u_B, u_T	Displacements, of bottom and top layers respectively, relative to x	τ	Shear stress
		τ'	First spatial derivative of τ

between the regions with and without delamination. The accuracy of the approach is verified by comparing results with previously published data.

2. Mathematical formulation

In the present work the delamination is modeled as a crack which separates the beam into a top (T) and bottom (B) layers. It is assumed that the delamination results in different transverse and axial displacements for the top and bottom layers.

Under these assumptions, the axial (U) and transverse (W) displacements for the top (T) and bottom (B) layers are written as

$$U_T(x, z) = u_T(x) - z \cdot w_T'(x) \tag{1}$$

$$U_B(x, z) = u_B(x) - z \cdot w_B'(x) \tag{2}$$

$$W_T(x, z) = W_T(x) \tag{3}$$

$$W_B(x, z) = W_B(x) \tag{4}$$

where a prime denotes differentiation with respect to x.

The strain relations for a piezoelectric layer (top) and beam (bottom) associated with the displacement field are given by

$$\varepsilon_T = u_T' - z \cdot w_T'' \tag{5}$$

$$\varepsilon_B = u_B' - z \cdot w_B'' \tag{6}$$

The piezoelectric constitutive equations, which neglect the thermal effects, can be expressed by [11–14]:

$$\sigma = \bar{\mathbf{Q}} \cdot \varepsilon - \bar{\mathbf{e}}^T \cdot \mathbf{E} \tag{7}$$

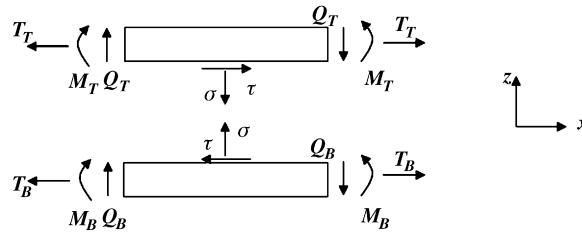$$\mathbf{D} = \bar{\mathbf{e}} \cdot \varepsilon + \bar{\mathbf{g}}^T \cdot \mathbf{E} \tag{8}$$

Fig. 1. Free-body diagram of an infinitesimal beam element with top and bottom layers.

For a beam problem, one can use $\sigma_y = \tau_{yz} = \tau_{xy} = 0$. The stress in the top and bottom layers is given by

$$\sigma_T = \bar{Q}_{11} \cdot \varepsilon_T - \tilde{e}_{31} \cdot E_z \tag{9}$$

$$\sigma_B = \bar{Q}_{11} \cdot \varepsilon_B \tag{10}$$

For the segment including the piezoelectric layer and the beam, the free-body diagram is shown in Fig. 1. From this figure the equation of motion can be derived as follows

$$\rho_T \cdot A_T \cdot \ddot{u}_T = T'_T + b \cdot \tau \tag{11}$$

$$\rho_T \cdot A_T \cdot \ddot{w}_T = Q'_T + b \cdot \sigma + P \tag{12}$$

$$M'_T + \frac{b \cdot h_T}{2} \cdot \tau - Q_T = 0 \tag{13}$$

$$\rho_B \cdot A_B \cdot \ddot{u}_B = T'_B - b \cdot \tau \tag{14}$$

$$\rho_B \cdot A_B \cdot \ddot{w}_B = Q'_B - b \cdot \sigma \tag{15}$$

$$M'_B + \frac{b \cdot h_B}{2} \cdot \tau - Q_B = 0 \tag{16}$$

where h_i $(i = T, B)$ denotes the thickness, b is the width of the beam, τ and σ are the shear and peel stress, T, Q and M are the axial stress resultant, transverse shear force and bending moment, respectively, A_i $(i = T, B)$ are the cross-section areas, P is the load per unit length, ρ_i $(i = T, B)$ are the mass densities of the layers.

The stress and the resultant moment in Eqs. (11)–(16) are

$$T_T = \bar{A}_T \cdot u'_T - \bar{B}_T \cdot w''_T - E_1 \tag{17}$$

$$M_T = \bar{B}_T \cdot u'_T - \bar{D}_T \cdot w''_T - E_2 \tag{18}$$

$$T_B = \bar{A}_B \cdot u'_B - \bar{B}_B \cdot w''_B \tag{19}$$

$$M_B = \bar{B}_B \cdot u'_B - \bar{D}_B \cdot w''_B \tag{20}$$

with

$$\bar{A}_T = \int_0^{h_2} \bar{Q}_{11} \cdot b \cdot dz; \qquad \bar{A}_B = \int_{-h_1}^0 \bar{Q}_{11} \cdot b \cdot dz \tag{21}$$

$$\bar{B}_T = \int_0^{h_2} \bar{Q}_{11} \cdot b \cdot z \cdot dz; \qquad \bar{B}_B = \int_{-h_1}^0 \bar{Q}_{11} \cdot b \cdot z \cdot dz \tag{22}$$

$$\bar{D}_T = \int_0^{h_2} \bar{Q}_{11} \cdot b \cdot z^2 \cdot dz; \qquad \bar{D}_B = \int_{-h_1}^0 \bar{Q}_{11} \cdot b \cdot z^2 \cdot dz \tag{23}$$

$$E_1 = \int_0^{h_2} \bar{e}_{31} \cdot b \cdot E_z \cdot dz; \qquad \bar{E}_2 = \int_{-h_1}^0 \bar{e}_{31} \cdot b \cdot E_z \cdot dz \tag{24}$$

Substituting Eqs. (17)–(20) into (11)–(16), the equation of motion will be

Table 1
Material parameters used in calculations.

x [m]	PZT-5H	Si
Q_{11} [10^{10} N/m^2]	12.6	16.6
Q_{12} [10^{10} N/m^2]	7.95	63.9
Q_{13} [10^{10} N/m^2]	8.41	63.9
Q_{33} [10^{10} N/m^2]	11.7	16.6
Q_{44} [10^{10} N/m^2]	2.3	79.6
Q_{66} [10^{10} N/m^2]	2.35	79.6
e_{31} [C/m^2]	−6.5	–
e_{33} [C/m^2]	23.3	–
e_{15} [C/m^2]	17.0	–
g_{11} [nF/m]	0.1503	0.1045
g_{22} [nF/m]	0.1503	0.1045
g_{33} [nF/m]	0.13	0.1045
ρ [kg/m^2]	7500	2330

Table 2
Deflections for the clamped-free beam.

x [m]	w [m] from FE	w [m] from present model	Error
0.000000	0.000000	0.000000	0.000000
0.033333	−2.216622e−4	−2.216622e−4	4.729826e−11
0.066667	−8.378124e−4	−8.378124e−4	4.949883e−11
0.100000	−1.780080e−3	−1.780080e−3	5.182010e−11
0.133333	−2.986606e−3	−2.986606e−3	5.420637e−11
0.166667	−4.402042e−3	−4.402042e−3	5.656910e−11
0.200000	−5.977553e−3	−5.977553e−3	5.876678e−11
0.233333	−7.670813e−3	−7.670813e−3	6.087850e−11
0.266667	−9.446009e−3	−9.446009e−3	6.291718e−11
0.300000	−1.127384e−2	−1.127384e−2	6.488764e−11
0.333333	−1.313152e−2	−1.313152e−2	6.669922e−11
0.366667	−1.500276e−2	−1.500276e−2	6.825461e−11
0.400000	−1.687780e−2	−1.687780e−2^2	6.941856e−11

$$\rho_T \cdot A_T \cdot \ddot{u}_T - \bar{A}_T \cdot u_T'' + \bar{B}_T \cdot w_T''' = -E_1' + k \cdot (b \cdot \tau) \tag{25}$$

$$\rho_T \cdot A_T \cdot \ddot{w}_T - \bar{B}_T \cdot u_T''' + \bar{D}_T \cdot w_T'''' = -E_2'' + k \cdot \left(\frac{b \cdot h_2}{2} \cdot \tau' + b \cdot \sigma \right) + P \tag{26}$$

$$\rho_B \cdot A_B \cdot \ddot{u}_B - \bar{A}_B \cdot u_B'' + \bar{B}_B \cdot w_T''' = k \cdot (b \cdot \tau) \tag{27}$$

$$\rho_B \cdot A_B \cdot \ddot{w}_B - \bar{B}_B \cdot u_B''' + \bar{D}_B \cdot w_B'''' = k \cdot \left(\frac{b \cdot h_1}{2} \cdot \tau' + b \cdot \sigma \right) \tag{28}$$

k is parameter characterizing the bonding conditions between the piezoelectric layer and the beam:

$k = 0$: Debonding

$k = 1$: Perfect bonding

3. Numerical results

In order to test the accuracy of the present work, several examples of beams with a piezoelectric actuator bonded as a top layer are considered.

In the first example a beam without delamination was considered and the results are compared to a finite element model [10]. The beam's length, width and thickness are $L = 0.4$ m, $b = 0.03$ m, and $h_B = 0.007$ m, the thickness of the piezoelectric layer is $h_T = 0.003$ m, a uniformly distributed load of 10^3 N m^{-2} is applied. The parameters of the beam and piezoelectric elements used in calculations are listed in Table 1.

The deflections for the clamped-free and clamped-clamped beams, as computed using Eqs. (21)–(24), are compared with those obtained by the use of an FE model [10]. In Tables 2 and 3, the results show that the deflections computed with the use of the present model are in good agreement with the finite element (FE) model results.

In the second example a beam with delamination between the top and bottom layers was considered. Figs. 2 and 3 show the axial displacement for the clamped-free and clamped-clamped beams, respectively.

Table 3
Deflections for the clamped-clamped beam.

x [m]	w [m] from FE	w [m] from present model	Error
0.000000	0.000000	0.000000	0.000000
0.033333	$-3.282879e{-}5$	$-3.282879e{-}5$	3.075542e–12
0.066667	$-1.085249e{-}4$	$-1.085249e{-}4$	3.009594e–12
0.100000	$-1.977867e{-}4$	$-1.977867e{-}4$	2.905288e–12
0.133333	$-2.778238e{-}4$	$-2.778238e{-}4$	2.692712e–12
0.166667	$-3.323576e{-}4$	$-3.323576e{-}4$	2.446617e–12
0.200000	$-3.516208e{-}4$	$-3.516208e{-}4$	2.281747e–12
0.233333	$-3.323576e{-}4$	$-3.323576e{-}4$	2.234577e–12
0.266667	$-2.778238e{-}4$	$-2.778238e{-}4$	2.243927e–12
0.300000	$-1.977867e{-}4$	$-1.977867e{-}4$	2.288599e–12
0.333333	$-1.085249e{-}4$	$-1.085249e{-}4$	2.260317e–12
0.366667	$-3.282879e{-}5$	$-3.282879e{-}5$	2.332458e–12
0.400000	0.000000	0.000000	0.000000
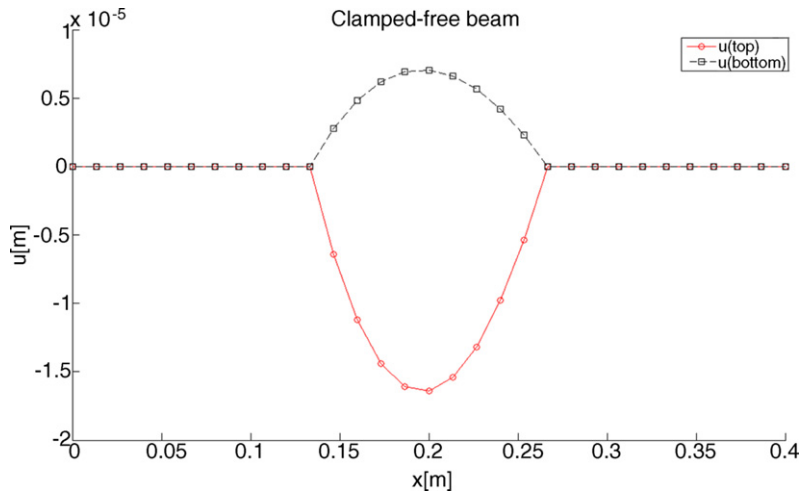
Fig. 2. Axial displacement for the clamped-free beam.
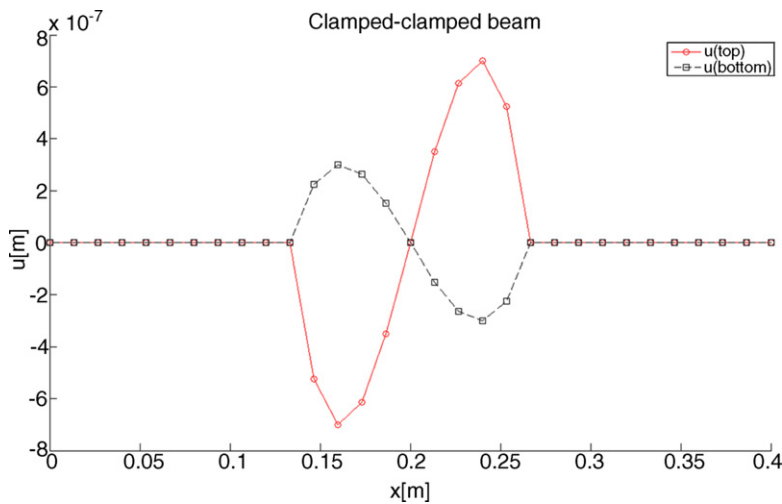
Fig. 3. Axial displacement for the clamped-clamped beam.

Figs. 4 and 5 show the axial displacement of the clamped-free beam for the top and bottom layers, respectively. It can be seen that their displacements increase with the thicknesses of the layers.

An electric voltage is applied to the actuator bonded on the top surface of host beam. The results of deflections for clamped-free beam are compared to those obtained for a beam without electric voltage application in Fig. 6. The results
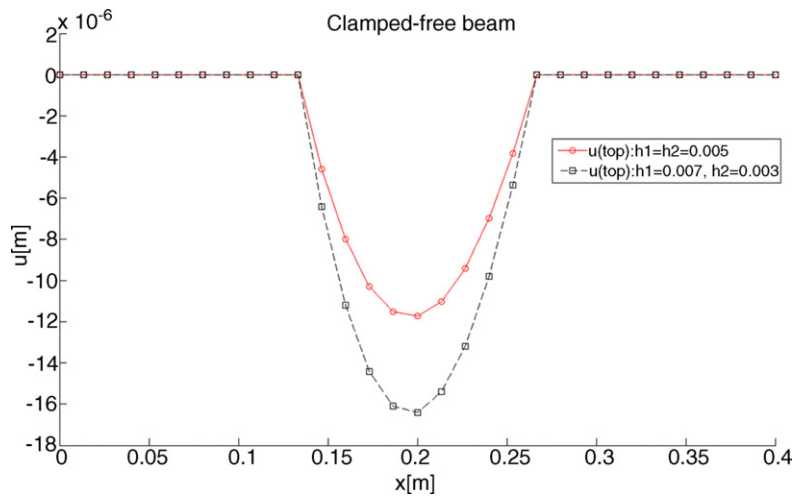
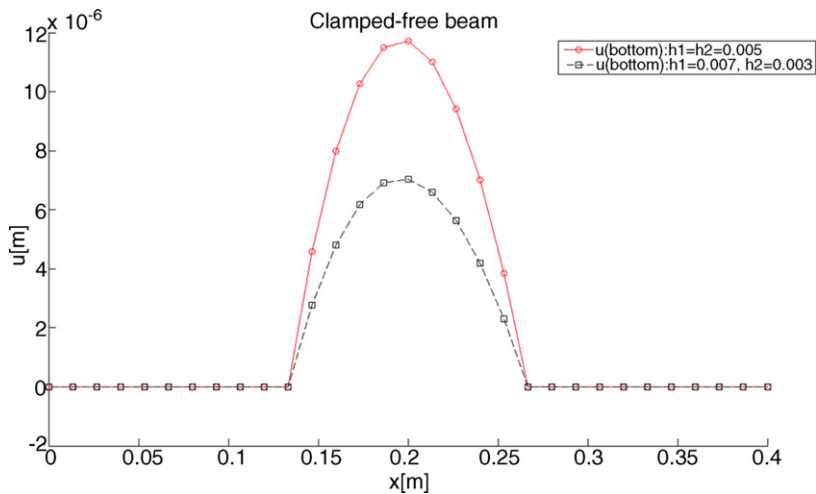**Fig. 4.** Axial displacement of top layer.

Fig. 5. Axial displacement of bottom layer.

Table 4
Natural frequencies for the clamped-free beam.

Mode	ν $(s-1)$ FE	ν $(s-1)$ present model	Error (%)
1	48.9255786	48.9243002	0.00
2	306.633498	306.352539	0.00
3	858.669041	856.666434	0.02
4	1682.55496	1675.51232	0.07
5	2781.36637	2762.91361	0.18
6	4154.88062	4114.91146	0.39

show that the behavior of the beam is affected by the delamination when a voltage input is applied to the piezoelectric layer.

The lowest 6 order natural frequencies computed with the present model are compared with the exact frequencies as shown in Table 4. The material and geometric characteristics are the same as in the previous example problems. The differences of the 1st- to the 6th-order natural frequencies are less than 0.4%.

4. Conclusion

A model of beams with delamination using Euler–Bernoulli beam theory is developed in this paper. Numerical results are presented to study the influence of delamination. The differences between the deflections computed from present model and previously computed data show that the results agree very closely. It is shown that the axial displacement increases
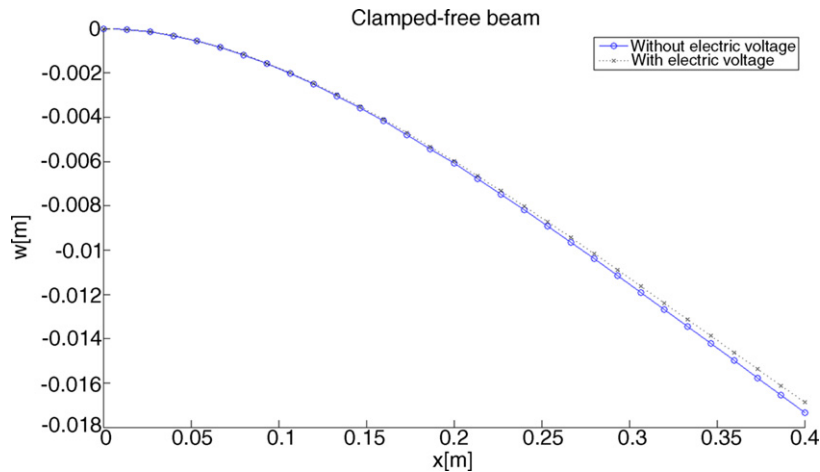
Fig. 6. Comparison of deflections with and without electric charge applied.

with the increasing of the thickness of layers. The frequencies computed with the model based on the formulation presented in this Note are in good agreement with the exact results. This shows the validity of the assumptions adopted in the present article.

References

[1] S. Yang, W. Huang, Piezoelectric constitutive equations for a plate shape sensor/actuator, AIAA Journal 35 (1997) 1894–1895.
[2] V. Piéfort, N. Loix, A. Preumont, Modeling of piezolaminated composite shells for vibration control, NASA/TM 1998-352487, 1998.
[3] B.K. Taleghani, J.F. Campbell, Non-linear finite element modeling of THUNDER piezoelectric actuators, NASA/TM 1999-245712, 1999.
[4] H.S. Tzou, M. Gadre, Theoretical analysis of a multi-layered thin shell coupled with piezoelectric shell actuators for distributed vibration controls, Journal of Sound and Vibration 132 (1989) 433–450.
[5] H.S. Tzou, A new distributed sensor and actuator theory for intelligent shells, Journal of Sound and Vibration 153 (1992) 335–349.
[6] S. Lee, T. Park, G.Z. Voyiadjis, Vibration analysis of multiple-delaminated beams, Composites Part B 33 (2002) 605–617.
[7] S.H. Kim, A. Chattopadhyay, A. Ghoshal, Characterization of delamination effect on composite laminates using a new generalized layerwise approach, Computers and Structures 81 (2003) 1555–1566.
[8] M.A. Hamed, A. Nosier, G.H. Farrahi, Separation of delamination modes in composite beam with symmetric delaminations, Materials and Design 27 (2006) 900–910.
[9] P. Tan, L. Tong, Delamination detection of composite beams using piezoelectric sensors with evenly distributed electrode strips, Journal of Composite Materials 38 (2004) 321–352.
[10] A. Mahieddine, M. Ouali, Finite element formulation of a beam with piezoelectric patch, Journal of Engineering and Applied Sciences 3 (2008) 803–807.
[11] E.F. Crawley, E.H. Anderson, Detailed models of piezoceramic actuation of beams, Journal of Intelligent Material Systems and Structures 1 (1990) 4–25.
[12] H.H. Law, P.L. Possiter, G.P. Simon, L.L. Koss, Characterization of mechanical vibration damping by piezoelectric materials, Journal of Sound and Vibration 197 (1996) 489–513.
[13] S.S. Rao, M. Sunar, Piezoelectricity and its use in disturbance sensing and control of flexible structures: A survey, Applied Mechanics Reviews 47 (1994) 113–123.
[14] B.T. Wang, R.A. Burdisson, C.R. Fuller, Optimal placement of piezoelectric actuators for active structural acoustic control, Journal of Intelligent Material Systems and Structures 5 (1994) 67–77.